

# DNA Binding Hairpin Polyamides with Antifungal Activity

Nicholas J. Marini,<sup>1,\*</sup> Ramesh Baliga,<sup>1</sup>  
Matthew J. Taylor,<sup>2</sup> Sarah White,<sup>1</sup>  
Paul Simpson,<sup>3</sup> Luong Tsai,<sup>1</sup>  
and Eldon E. Baird<sup>2,4,\*</sup>

<sup>1</sup>Department of Microbial Genomics

<sup>2</sup>Department of Synthetic Chemistry

<sup>3</sup>Department of Pharmacology

GeneSoft, Inc.

South San Francisco, California 94080

## Summary

Eight-ring hairpin polyamides containing N-methylimidazole (Im) and N-methylpyrrole (Py) amino acids have been shown to bind with subnanomolar affinity to discrete DNA sites and to modulate a variety of DNA-dependent biological processes. We show here that addition of a second positive charge at the C terminus of an 8-ring hairpin polyamide confers activity against a number of clinically relevant fungal strains *in vitro*, and activity against *Candida albicans* in a mouse model. Control experiments indicate that the observed antifungal activity results from a DNA binding mechanism-of-action that does not involve DNA damage or disruption of chromosomal integrity. Hairpin activity is shown to be proportional to yeast DNA content (ploidy). Transcriptional interference is proposed as the likely explanation for fungal cytotoxicity. Experiments with sensitized yeast strains indicate the potential for discrete sites of action rather than global effects.

## Introduction

The natural product distamycin (Py-Py-Py+) was first discovered by Arcamone and coworkers over 40 years ago [1, 2]. This crescent-shaped synthetic compound containing three pyrrole amino acids was found to bind DNA in the minor groove and to inhibit DNA-dependent processes, including transcription [3]. Distamycin has modest antibacterial [4], antimalarial [5], antifungal [6], and antiviral activities [7], but is limited to topical use because of toxicity [8]. Recent efforts to bring an optimized distamycin to the clinic have focused on small synthetic analogs for use as antibacterial [9, 10], antifungal [11], or antimalarial therapeutics [12]. These analogs generally have been optimized for pathogen activity as well as pharmacological properties, with DNA binding affinity and specificity not providing a major driving force in compound design or selection.

Separate work has focused on controlling the DNA binding sequence specificity of minor groove binding ligands [13–14]. For example, larger analogs such as hairpin polyamides (distamycin has a MW of 518, a typi-

cal 8-ring hairpin has a MW of 1222) use a side-by-side pairing scheme in the minor groove [15], and a broadened heterocycle amino acid repertoire to bind to specific predetermined DNA sequences according to a ring-pair:base-pair code [16–18]. A variety of templates have been developed to use the pairing code for recognition of sites from 6–16 base pairs [19, 20]. One useful motif is the eight-ring hairpin polyamide class containing N-methylimidazole (Im) and N-methylpyrrole (Py) amino acids, which bind to discrete sites with subnanomolar affinities [21]. These compounds have been shown to modulate transcription *in vitro* and viral replication in human cells [22, 23]. However, uptake of hairpin compounds may currently be limited to certain cell types [24].

The question that we address here is to determine if the hairpin compounds, with their greater potential for rational sequence targeting, can be used against anti-infective targets in microorganisms. We report chemical principles for conferring antifungal activity on hairpin polyamides and begin to assess mechanism-of-action. Our data indicate that activity is mediated by a reversible interaction with chromosomal DNA that does not induce DNA damage and may interfere with transcription of a discrete set of genes.

## Results and Discussion

### Chemistry

All compounds were synthesized by stepwise Boc-chemistry solid phase methods [25] and isolated as the acetate salts using 0.1% acetic acid in the HPLC mobile phase. Hairpins containing a single dimethylaminopropylamino (Dp) tail were synthesized on Boc-β-PAM-resin (β = β-alanine); hairpins with two Dp tails were prepared on Boc-D-Asp(OBzl)-PAM resin. The Dp tail(s) was introduced during the final aminolysis/resin cleavage step, which substitutes the PAM carboxylic ester as well as the β-carboxybenzyl ester. In this way, identical solid phase cycles utilizing two different starting resins produced the compounds shown in Figure 1.

### DNA Binding Effects

Compound 1 ImPyPyPy-γ-PyPyPyPy-β-Dp (γ = γ-aminobutyric acid) and Compound 2 ImPyPyPy-γ-PyPyPyPy-Asp-(Dp)-Dp are predicted to bind to a 5'-WWGWWW-3' binding site (W = A or T); Compound 3, ImPyPyPy-γ-ImPyPyPy-β-Dp, and compound 4, ImPyPyPy-γ-ImPyPyPy-Asp-(Dp)-Dp are predicted to bind to a 5'-WWGWWCW-3' target site. DNase I footprinting revealed that Hairpin 2, which contains 2 Dp residues at the C terminus, has an approximate 10-fold reduction in DNA binding affinity for a 5'-ATGTATT-3' match site relative to the singly substituted parent compound (Figure 1). Compound 4 also has a 10-fold reduction in binding affinity relative to compound 3 for its 5'-ATGTACT-3' match site. Affinity at the 5'-ATGTATT-3' (mismatch base pair underlined) single base pair mismatch site is also reduced by 10-fold for compound 4 relative

<sup>4</sup>Present address: Oakwood Products, Inc., West Columbia, SC 29172

\*Correspondence: nmarini@att.net; ebaird@oakwoodchemical.com

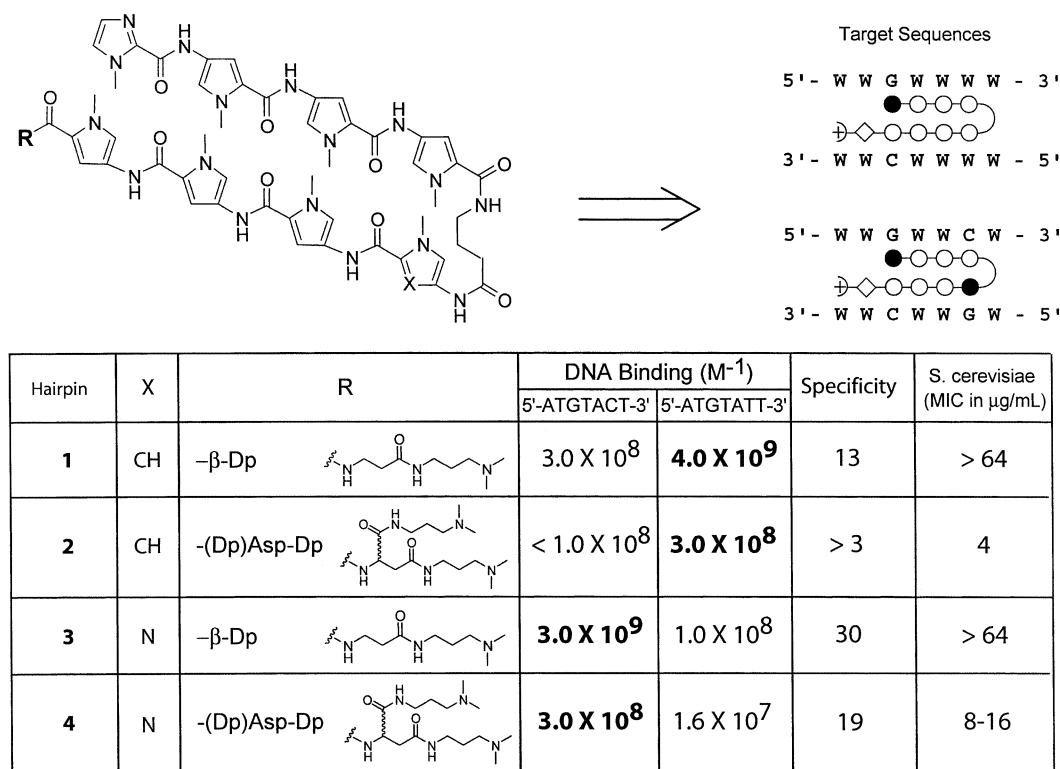


Figure 1. Structures and Schematic Models of Eight-Ring Hairpin Polyamides

ImPyPyPy- $\gamma$ -PyPyPyPy- $\beta$ -Dp (1), ImPyPyPy- $\gamma$ -PyPyPyPy-(Dp)Asp-Dp (2), ImPyPyPy- $\gamma$ -ImPyPyPy- $\beta$ -Dp (3), and ImPyPyPy- $\gamma$ -ImPyPyPy-(Dp)Asp-Dp (4). Filled and open circles represent imidazole (Im) and pyrrole (Py) polyamide rings, respectively, targeted to their match DNA base pairs. A diamond represents the C-terminal  $\beta$ -amino acid ( $\beta$ -carboxamido Asp or  $\beta$ -alanine) and a plus sign represents the charged dimethylaminopropylamido (Dp) tail (2-Dp for Asp, 1-Dp for  $\beta$ -alanine).  $\gamma$ -Aminobutyric acid ( $\gamma$ ) is depicted by a curved line. Equilibrium association constants ( $K_a$ ) for each polyamide binding to the indicated match (indicated in bold) and mismatch sites were determined by DNase I footprinting. Specificity was determined by the ratio of the resulting binding constants ( $[K_a \text{ match site}]/[K_a \text{ mismatch site}]$ ). In vitro susceptibility testing (MIC) for *Saccharomyces cerevisiae* was conducted by the NCCLS broth microplate assay in 100  $\mu\text{l}$  volumes in 96-well plates in YPD media. It should be noted that the mismatch site  $K_a$  reported for compound 2 (<  $1 \times 10^8 M^{-1}$ ) represents a lower limit, as the DNase titration was only carried up to 10 nM concentration and was not repeated.

to compound 3; thus, specificity is relatively unchanged (reduced by about a factor of 2), 30-fold for compound 3 and 19-fold for compound 4. For compound 2, footprint titration experiments were only run at concentrations < 10 nM; thus, we can only report a lower limit for specificity of compound 2. For the design of DNA binding hairpins, this work adds to the knowledge of acceptable tail groups that can be accommodated at the C termini of hairpin polyamides. To summarize, Py-Dp and Py- $\beta$ -Dp [26], and the Py-Asp(Dp)-Dp termini reported here, provide hairpins with comparable DNA binding specificity (at least for sites adjacent to an A or T base pair) [27], but Py-Gly-Dp [26] and Py- $\gamma$ -Dp (unpublished data) show greatly reduced binding specificity, perhaps due to an increased preference for binding in the 5'-3' C-N reverse binding orientation [28, 29]. (We should note that the stereochemistry of the C-terminal Asp residue was not confirmed in these studies. We observe similar DNA binding affinities and similar biological effects when compounds are made from D-Asp-resin and from L-Asp-resin, which could indicate that the stereochemistry is not important for the DNA binding, or that the resin cleavage chemistry results in interconversion.) Given the large differences in binding affinity and specificity

observed for compounds that differ from  $\beta$ -Dp to Gly-Dp at the C terminus, addition of the second Dp-carboxamide residue results in a surprisingly small difference in the DNA binding properties of these compounds. These results indicate that correct placement of the terminal amide in the minor groove may be more significant for binding specificity (avoiding reverse orientation) than steric effects on the tail.

#### In Vitro Activity of Hairpin Polyamides

The singly charged parent compounds 1 and compound 3 show no antifungal activity, even at concentrations greater than 64  $\mu\text{g/ml}$  (50  $\mu\text{M}$ ) (the solubility of the 8-ring hairpins in water is approximately 100  $\mu\text{M}$ ). Addition of the second Dp residue to provide the doubly charged compounds 2 and 4 results in dramatically improved in vitro antifungal activity (based on susceptibility of *Saccharomyces cerevisiae*), with an MIC of 4  $\mu\text{g/ml}$  observed for compound 2 and an MIC of 8–16  $\mu\text{g/ml}$  observed for compound 4 (Figure 1). Although the reasons for this increase in activity are not yet clear, a likely explanation is that addition of the second Dp moiety improves the uptake properties of the compounds. If

**A**

Organism	MIC ( $\mu\text{g/mL}$ )
<i>C. albicans</i> (ATCC 90028)	4
<i>C. neoformans</i> (ATCC 90112)	2
<i>C. parapsilosis</i> (ATCC 10232)	1
<i>C. tropicalis</i> (ATCC 13803)	4
<i>S. cerevisiae</i> (BY4741)	4
<i>A. niger</i> (ATCC 10535)	> 64

**B**

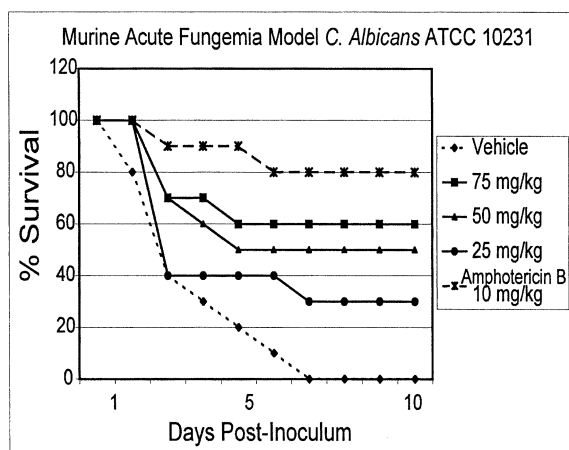


Figure 2. In Vitro and In Vivo Activities of Hairpin Polyamide 2, ImPy PyPy- $\gamma$ -PyPyPyPy-Asp(Dp)-Dp

(A) In vitro susceptibility testing (MIC). All strains were tested using the broth microdilution plate method according to NCCLS guidelines (see Experimental Procedures).

(B) In vivo activity was measured in a murine acute fungemia model. Groups of 10 mice were inoculated intravenously with  $10^7$  CFU *Candida albicans* per mouse. Compound 2 or Amphotericin B were administered intraperitoneally (IP) one hour after fungal inoculation. Mortality was recorded once daily for 10 days.

so, these results suggest that improved uptake can overcome a reduction in DNA binding affinity.

We tested doubly charged hairpin polyamides on several clinically relevant fungal pathogens in order to further explore the spectrum of cytotoxicity. Figure 2A shows the minimal inhibitory concentration (MIC) from in vitro susceptibility testing on several yeast-like pathogens (*Candida albicans*, *Candida parapsilosis*, *Candida tropicalis*, *Cryptococcus neoformans*) as well as a filamentous fungus (*Aspergillus niger*) for compound 2. Interestingly, compound 2 is also active against a variety of yeast-like pathogens with similar potencies as measured against *Saccharomyces cerevisiae*. Compound 2

was significantly less active against *Aspergillus* or other filamentous fungi (data not shown). Although the cellular basis for the different behavior in budding versus filamentous fungi is not understood, this is a common feature of antifungal therapies (e.g., flucytosine, fluconazole) and is probably related to cellular uptake/permeability [30]. Compound 4 was also active against the same panel of pathogens, but with decreased potency similar to that seen with *S. cerevisiae*.

**In Vivo Activity of Antifungal Hairpin Polyamides**

We also tested compound 2 for in vivo efficacy in a mouse model of acute fungal infection (Figure 2B). In this study (see Experimental Procedures for details), compound 2 or the positive control amphotericin B were injected into mice shortly after i.v. administration of a lethal dose ( $\text{LD}_{90-100}$ ) of *Candida albicans*. Efficacy is measured by mouse protection over time. In this animal model, compound 2 displayed significant efficacy in a dose-dependent fashion. Thus, compound 2 has sufficient potency, stability, and bioavailability to be active in vivo. It should also be noted that acute rodent toxicity testing at these same doses indicated that compound 2 is well tolerated (100% survival; no significant changes in serum chemistry or behavior/appearance; data not shown). Hairpin compound 2 showed excellent metabolic stability in serum and in liver microsomes (data not shown), indicating that the observed activity is resulting from the intact hairpin, and not from a smaller metabolite. Based on in vitro potency, in vivo activity, and lack of acute toxicity, hairpin polyamides may have potential as novel mechanism-of-action antifungal agents.

**Dependence of Antifungal Activity on Genomic DNA Content and DNA Recognition Site**

To better understand the underlying mechanism behind antifungal activity, we investigated the interaction between hairpin polyamides and yeast chromosomal DNA. First, to verify that DNA was indeed the target through which fungal cytotoxicity was mediated, we tested whether increasing genomic DNA content could reduce susceptibility. It has been demonstrated previously that increasing gene dosage of a drug target increases resistance of *Saccharomyces cerevisiae* to the corresponding drug by requiring higher effective concentrations to overcome target function [31, 32]. Thus, if the genome was the key target, either globally or a discrete subset, increasing the dosage of the genome (by increasing the complement of chromosomes or ploidy) should confer increasing resistance to hairpin polyamides. The rationale is that increases in ploidy should increase the cellular concentration of DNA target sites and, therefore, require higher intracellular concentrations of compound to achieve critical occupancy at those sites.

Figure 3A shows growth on MIC-determination plates for haploid (1n), diploid (2n), and tetraploid (4n) strains of *Saccharomyces cerevisiae* in the presence of compound 2. MIC for these strains clearly increases in proportion to ploidy or genomic DNA content: 4  $\mu\text{g/ml}$  for haploids, 8  $\mu\text{g/ml}$  for diploids, and 16  $\mu\text{g/ml}$  for tetraploids. In control experiments, a similar dependence on ploidy is seen for other compounds that kill via chromo-

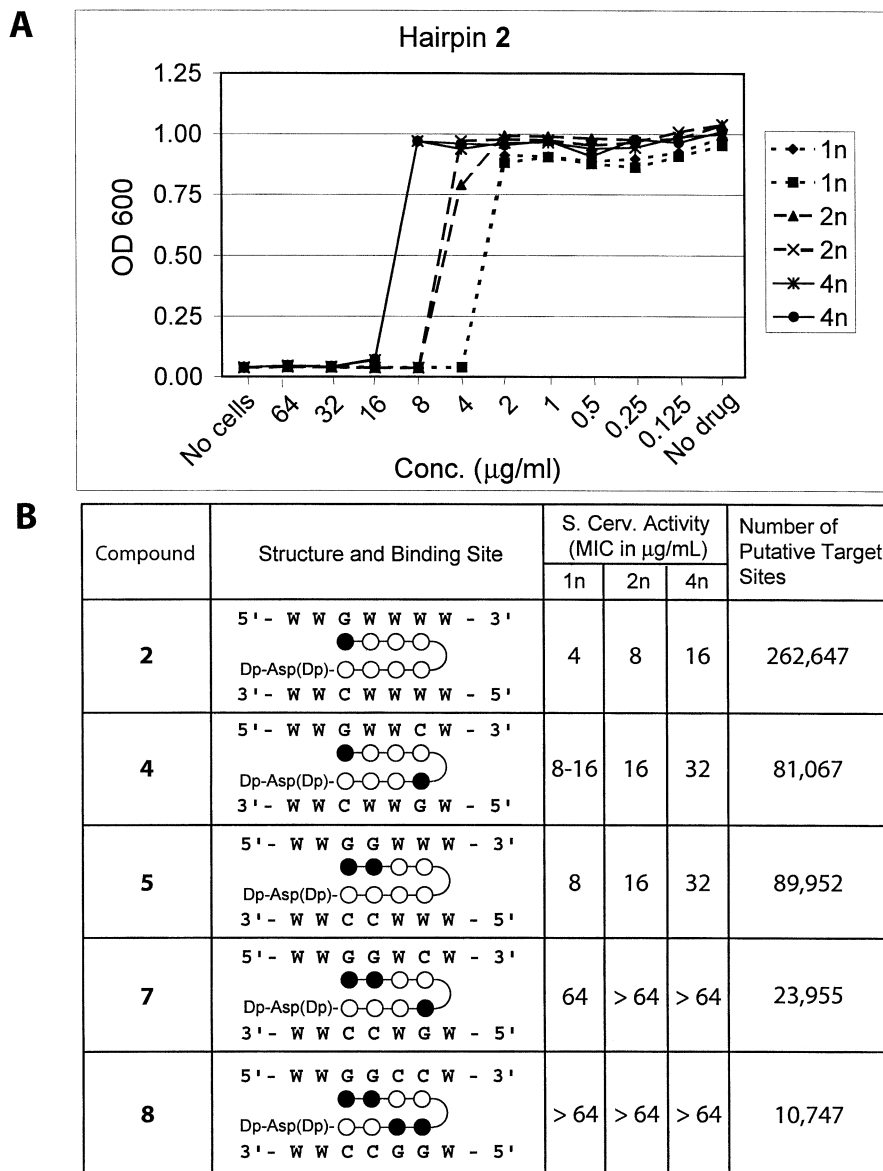


Figure 3. Effects of Yeast Genomic Content (Ploidy) on Activity of a Series of Hairpin Polyamides with Increasing G,C Content in their Target Sites

Susceptibility of *S. cerevisiae* strains to antifungal polyamides was measured by the broth microdilution assay exactly as in Figure 2. Haploid (1n), Diploid (2n), and Tetraploid (4n) yeast were tested in duplicate.

(A) Optical density of a test plate showing growth in the presence of compound 2.

(B) Compound series with increasing 1m substituents and, therefore, GC content in the binding site. Number of theoretical binding sites in the *Saccharomyces* genome was obtained using the PatMatch search engine on the *Saccharomyces* Genome Database (SGD) web server (<http://genome-www.stanford.edu/Saccharomyces>).

somal DNA binding, such as the alkylator methyl methane sulfonate (MMS), but not for compounds with an enzymatic or other non-DNA target such as clotrimazole (data not shown). Titration of the potency of compound 2 by genomic DNA suggests that chromosomes are the actual target and that antifungal activity is through a DNA binding mechanism.

To assess the role of the recognition site programmed into the polyamide, a series of compounds was synthesized that recognize different target sites with increasing G,C content relative to compound 2. As shown in Figure

3B, increasing the number of 1m/Py pairings decreases potency against *S. cerevisiae*. Nevertheless, where activity is observed, it is dependent on chromosomal DNA content with a doubling of the chromosome number resulting in a 2-fold increase in MIC as in Figure 3A.

One explanation for the decreased potency of compounds with increasing G,C target site content is highlighted in the last column of Figure 3B. The predicted binding site for each compound was scanned against the *Saccharomyces* genome sequence (see figure legend), and the number of hits is indicated. 7-bp predicted

binding sites were used for this search, based on known end effects for hairpin polyamides [27]. There are progressively fewer target sites in the genome for compounds that recognize sequences with increasing GC content. Thus, whether compound binding causes more global chromosome perturbations (e.g., interference with chromosome topology [33]) or more discrete events (e.g., interference with transcription of specific genes [22]), the likelihood that a binding event(s) results in a deleterious outcome increases with its frequency along the chromosome. If binding events are roughly dictated by the predicted match sequences shown in Figure 3B, one would predict that each compound might have different aspects of mechanism, since the overall binding patterns would be different.

A second possibility, however, is that there is a defined set of key target sites which are better recognized by hairpins that bind to sequences of the form 5'-WWGWWW-3' or to A,T-rich sequences in general. In this case, overall binding patterns, and therefore mechanism, might be the same, with potency simply being a reflection of compound affinity for the target sites. Still a third possibility is some combination of sequence-driven and affinity-driven effects. As shown below, this last possibility may most closely approximate the true mechanism.

#### DNA Damage-Sensitive Yeast Are Not Hypersensitive to Compound 2

Hairpin polyamides like compounds 1–8 reversibly bind DNA *in vitro* [13, 14]. Since these compounds appear to be acting via a DNA-based mechanism *in vivo*, we wished to verify that lethality was not a result of DNA damage or chromosome breakage. DNA damaging activity might provide a toxicity hurdle for developing antifungal therapeutics (although all acute animal toxicity testing has shown excellent tolerability; see above).

We tested compound 2 on *S. cerevisiae* mutant strains that are hypersensitive to various perturbations of chromosomal integrity (Figure 4). *RAD9* and *MEC1* encode genes whose products function in checkpoint pathways that monitor genomic integrity or incompletely replicated DNA. These pathways negatively feed back on cell cycle progression so as to give the cell the opportunity to repair any defects before catastrophic events occur at mitosis. In the absence of these functions, cells become hypersensitive to agents that disrupt chromosomal integrity (e.g.,  $\gamma$ /UV irradiation, radiomimetic drugs, Hydroxyurea), since the cell no longer has the opportunity for repair (reviewed in [34]).

The top panel of Figure 4 shows that mutant strains defective in either Rad9p or Mec1p function displayed increased sensitivity (decreased MIC) to the radiomimetic drug methyl methane sulfonate (MMS). This increase is consistent with previous results, which showed increased sensitivity to MMS for *rad9* mutants [35] as well as a Mec1-dependent activation of the S phase checkpoint and concomitant slowing of chromosomal DNA replication [36]. In contrast, no change in activity was seen between the mutant and wild-type strains for compound 2.

This result suggests that compound 2 binds reversibly and does not induce DNA damage or chromosome

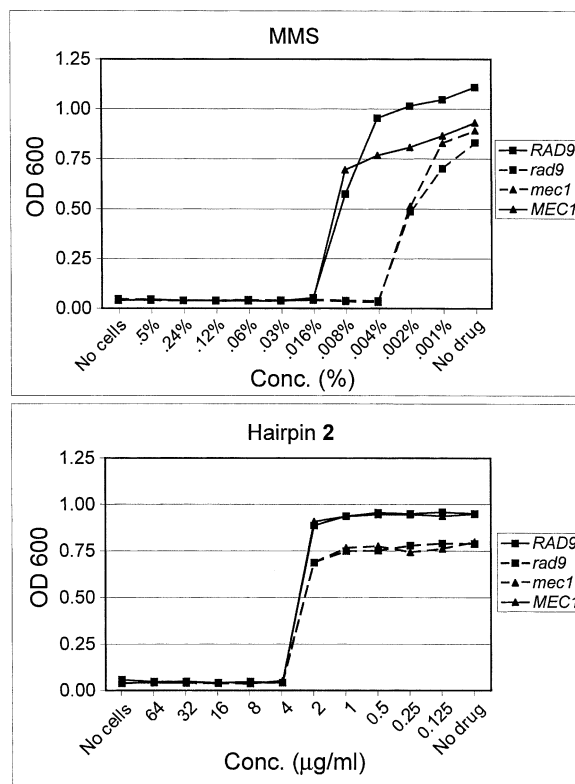


Figure 4. Susceptibility of *S. cerevisiae* Strains to Compound 2 or Methyl-Methane-Sulfonate (MMS) Was Measured by the Broth Microdilution Assay as in Figure 2

Two DNA damage-sensitive mutants (*rad9*, *mec1*) and their congenic wild-type strains (*RAD9*, *MEC1*) were tested. Optical densities are from a test plate showing growth of in the presence of MMS or compound 2.

breakage. In addition, the antifungal effects of compound 2 are probably not entirely mediated via global changes in chromosome structure such as topology/supercoiling, replication, or segregation, since interference with these processes would score positive in this assay [34–36]. Therefore, the primary mechanism by which hairpin polyamides effect yeast cell death may be to interfere with the use of chromosomal DNA as a template for gene transcription [22].

#### Validation of the *S. cerevisiae* Hypersensitivity Growth Assay to Identify Antifungal Compound Targets

If transcriptional interference is the primary activity of antifungal polyamides, the question arises as to whether interference is global across the genome or occurs at more specific sites of action. In a comprehensive hunt for polyamide targets/sites-of-action, we employed a genomic approach to assay all *Saccharomyces* essential genes for the potential of polyamide intervention. The assay measures drug hypersensitivity in target-compromised cells based on a previously reported method that has been successfully used to identify antifungal drug targets [37]. Decreased gene dosage of a drug target from two copies to one copy in heterozygous

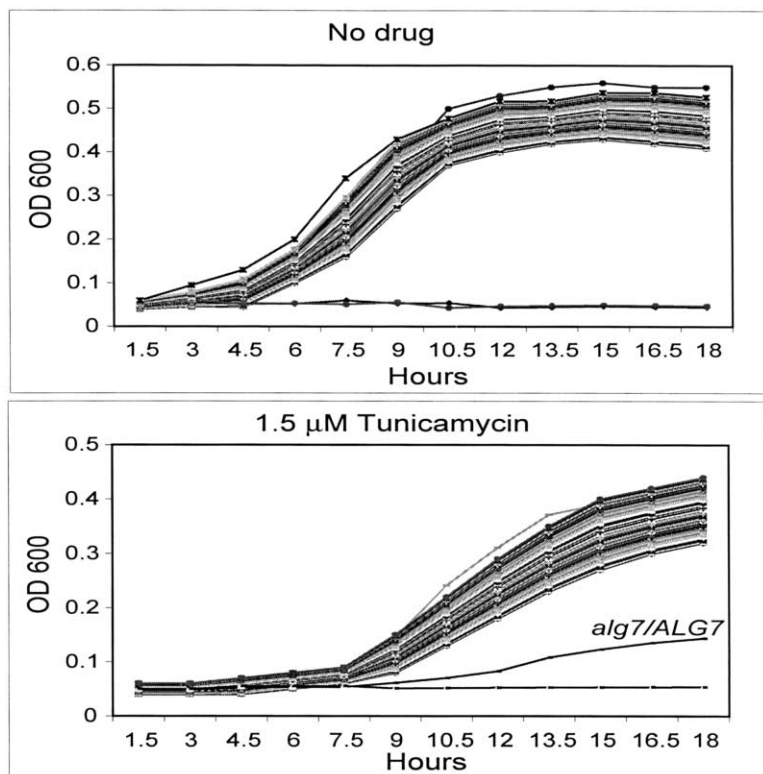


Figure 5. Diploid Yeast Cells Heterozygous for a Target Gene (*ALG7*) Display Greater Sensitivity to Tunicamycin than Nontarget Heterozygotes

Growth curves are for a single 96-well plate that contains 94 representative yeast strains heterozygous for different essential genes plus 2 media blanks. The strains were chosen at random, but to include the primary tunicamycin target gene *ALG7*. The upper graph shows overlapping growth curves for all 94 strains in rich media in the absence of drug. The lower graph shows growth in the presence of a sublethal dose of the test compound tunicamycin (1.5  $\mu$ M).

yeast strains results in increased sensitivity to that cognate drug. In the heterozygous cell, the target becomes more rate-limiting for growth in the presence of a sublethal concentration of drug due to the reduction in copy number by 50%.

We modified the assay format to assess drug hypersensitivity by scoring growth rates in 96-well plates (see Experimental Procedures for details). A plate assay enabled us to scan all essential gene heterozygotes in parallel by simply measuring turbidity over time. To validate the assay, we first performed a feasibility study using a well-characterized antifungal compound, tunicamycin. Tunicamycin specifically targets Asn-linked glycosylation, thus preventing proper modification of secreted proteins [38, 39]. Figure 5 shows the results from a prototypical 96-well plate carrying 94 different *Saccharomyces* essential gene heterozygotes. Strains were inoculated from stationary phase at  $t = 0$ . The upper graph shows overlapping growth curves for all 94 strains in rich media in the absence of drug. The lower graph shows growth in the presence of a sublethal dose of the test compound tunicamycin (1.5  $\mu$ M). Note that growth is slowed for all strains due to the effects of intermediate tunicamycin treatment. The strain heterozygous for the tunicamycin target (*alg7/ALG7*) displays significantly slower growth and greater sensitivity due to combined effect of intermediate tunicamycin treatment and the lower copy number of *ALG7*. These results are consistent with previous studies [37–39] identifying the *ALG7* locus as a tunicamycin target. Based on tunicamycin as a validating example, putative antifungal targets can be identified by determining which heterozygous loci show this drug-induced hypersensitivity [37].

#### Differential Sensitivity of Yeast Heterozygotes to a Pair of Antifungal Polyamides with Different Sequence Specificity

A panel of 743 *Saccharomyces* essential gene heterozygotes was assayed for hypersensitivity as in Figure 5 in the presence of tunicamycin, compound 2, and compound 5. This collection represents approximately 75% of all yeast essential genes. Growth rates were measured and only those strains that scored as hypersensitive are plotted in Figure 6. Growth defects of the affected strains were semiquantitatively assigned as mild, moderate, or severe (see Experimental Procedures for details).

As shown in Figure 6, there was one heterozygote strain (*PRS1*) that showed increased sensitivity to all compounds, indicating nonspecific effects due to the overall poor health of cells with decreased *PRS1* function. Only the *PRS1* strain in the collection displayed such nonspecific behavior.

Tunicamycin affected 8 strains uniquely: the target *ALG7* as well as other mutations in the secretory pathway (*CDC24*, *PBN1*) [40–42]. This observation highlights the point that this approach may also identify other rate-limiting steps in the target pathway. In addition, there were 5 strains not obviously involved in N-linked glycosylation or secretion (*PTA1*, *TIF11*, *SRB6*, *CBF2*, *RPC10*). Although it is not yet clear why deficiencies in these functions lead to tunicamycin hypersensitivity, they may represent downstream or secondary effects from defects in glycosylation or secretion (see also [37]).

To summarize the hairpin polyamide results, outside of *PRS1*, a total of 15 strains displayed hypersensitivity to compound 5 (5'-WWGGWWW-3' target site) and 17 strains hypersensitivity to compound 2 (5'-WWGWWW-

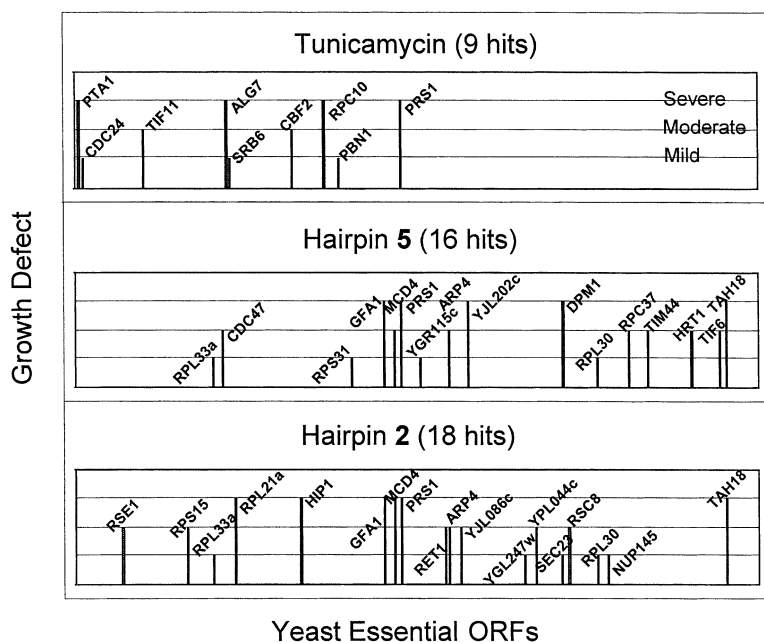


Figure 6. A Panel of *S. cerevisiae* Essential Gene Heterozygotes was Screened as in Figure 5 Against Tunicamycin, Compound 2, and Compound 5

743 strains were tested in duplicate at multiple sublethal concentrations of each compound; thus, the x axis contains 743 categories for each heterozygote strain in the collection. Hypersensitive strains were assessed as having mild, moderate, or severe growth defects (see Experimental Procedures), and only those are indicated.

3' target site). Out of these, there were 6 strains hit by both compounds 2 and 5 (*RPL33A*, *GFA1*, *MCD4*, *ARP4*, *RPL30*, *TAH18*); Compound 5 affected 9 strains uniquely, while Compound 2 targeted 11 strains uniquely.

Thus, it appears that only a relatively small number of essential gene functions are sensitive to both compounds 2 and 5. If binding events that produced a functional outcome were widespread across the genome, one might expect a more global response in this type of assay. Instead, the profile of sensitized strains indicates a level of specificity that approximates tunicamycin, an agent with a specific cellular target. The nature of such specificity is not currently known. For example, only a subset of putative genomic binding sites may be occupied at growth inhibitory concentrations, or only a subset of binding events may affect a biological outcome.

Looking at the gene functions affected by antifungal polyamides reveals no obvious biological theme. One would not necessarily expect one, however, if compounds act via DNA binding. The only common feature necessary would be binding site attributes such as sequence and position, not function. We have done some preliminary sequence analysis at the affected loci (site frequency, positioning, clustering), but have not seen any striking common features. Clearly, more work is needed to elucidate compound behavior in vivo and molecular mechanisms of action.

Both compounds share a common response pattern indicating similar aspects of mechanism, as well as targets unique to each compound. The similar responses could be a reflection of key target sites recognized by both compounds, though perhaps with unequal affinities, since compound 2 is more potent than compound 5. The unique responses could be a reflection of altered sequence specificity that programs a different set of discrete events. These data suggest some degree of specificity with respect to gene inactivation.

Although we do not yet have a full explanation for these observations and the molecular basis of specificity, many of the findings we report here are in good agreement with a previous report studying hairpin polyamide:DNA interactions in mammalian cells [43]. Using microarray analysis to determine polyamide effects on mRNA expression, these authors concluded that although putative match binding sites are found widely in the genome, only a relatively small number of genes were targeted transcriptionally in the cell. In addition, there did not seem to be a common theme regarding matched polyamide target sites with respect to clustering, positioning, or flanking sequence context in the promoters of these affected genes (although affected gene promoters did contain matched binding sites). In fact, the specific gene that was the intended target of the designed polyamides was unaffected. The authors also noted that small changes in polyamide structure led to differences in transcriptional effects similar to what we see in the yeast heterozygote screening (Figure 6). Finally, polyamide treatment did not induce DNA damage reporters, but rather downregulated them, indicating the absence of measurable DNA damage, which is again consistent with our finding that DNA damage-sensitive yeast mutants are not hypersensitive to these compounds (Figure 4).

These findings indicate that we do not yet fully understand the rules for predicting genomic effects of polyamide treatment based on rational design. A genomic approach to this problem should be informative in conjunction with studies elucidating biochemical and biophysical parameters of these compounds. In this regard, *Saccharomyces cerevisiae* is an ideal organism in which to learn more about polyamide behavior at the cellular level. We have already established rules to achieve cell penetration and nuclear activity. Furthermore, *S. cerevisiae* is an excellent eukaryotic cell model with a small, well-characterized genome and a multitude

of genetic and genomic tools to call upon. As shown here, we have begun to employ this approach for polyamides within the antifungal arena, but these studies should be enlightening in a broader context.

## Significance

Eight-ring hairpin polyamides containing N-methylimidazole (Im) and N-methylpyrrole (Py) amino acids have been shown to bind with subnanomolar affinity to discrete DNA sites and to modulate a variety of DNA-dependent biological processes. We show here that addition of a second positive charge at the C terminus of an 8-ring hairpin polyamide confers activity against a number of clinically relevant fungal strains *in vitro*, and activity against *Candida albicans* in a mouse model. Antifungal activity is modulated by the ploidy of the yeast, with increasing genome copy numbers (cellular DNA content) leading to a corresponding reduction in hairpin antifungal activity. Increasing G,C content within the hairpin target site decreases antifungal activity in a manner proportional to the predicted number of hairpin binding sites in the *Saccharomyces* genome. DNA damage-sensitive yeast strains show no increase in sensitivity to the hairpin polyamides, indicating that the critical DNA binding events are reversible. Even though the compounds in this study are predicted to bind to many sites within the yeast genome, experiments performed with a panel of heterozygote mutant yeast strains indicate that a discrete number of genes/gene functions are affected by the compounds. This indicates that the antifungal activity may result from interference with only a limited subset of genes. These results taken together indicate a potential DNA binding mechanism-of-action for the observed antifungal activity, demonstrating that these compounds may have potential as novel mechanism-of-action antifungal agents. Overall, we have developed general chemical principals for conferring antifungal activity on hairpin polyamides, which should encourage the further use of yeast systems for understanding polyamide behavior at the cellular level.

## Experimental Procedures

### Reagents and Media

Boc- $\beta$ -alanine PAM resin (substitution 1.1 mmol/gram) was purchased from Peptides International. Boc-D-Asp(OBzl)-PAM resin (substitution 0.5 mmol/gram) was purchased from NovaBiochem. Imidazole-2-carboxylic acid, Boc-4-aminoimidazole-2-carboxylic acid, and Boc-4-aminopyrrole-2-carboxylate OBt ester were purchased from Oakwood Products, Inc. RPMI-1640 growth media, methyl-methane sulfonate (MMS), tunicamycin, and clotrimazole were purchased from Sigma. Potato dextrose agar was purchased from Remel. YPD media is 1% yeast extract (Difco), 2% peptone (Difco), 2% dextrose (Sigma).

### Chemistry

Compounds were synthesized stepwise by established solid phase methods from either Boc- $\beta$ -alanine PAM resin or Boc-D-Asp(OBzl)-PAM resin [25]. Aminolysis (including substitution of the  $\beta$ -carboxybenzyl ester with Dp) was performed with neat dimethylaminopropylamine (Dp) (2 ml for 0.5 gram resin) at 60°C for 12 hr. The resulting solution was purified by reverse HPLC using a Hamilton PRP-1 divinylbenzene 250  $\times$  50 mm column with a gradient elution (buffer A: 0.5% aqueous acetic acid, buffer B: acetonitrile; 0%–60% B over 120 min at a flow rate 20 ml/min). Correct fractions were identified by

electrospray mass spectroscopy (LCQ Finnigan mass spectrometer) and were lyophilized to an off-white powder. NMR determinations were made on a Varian 400 MHz spectrometer.

### Compound 2 ImPyPyPy- $\gamma$ -PyPyPyPy-Asp(Dp)-Dp

<sup>1</sup>H NMR (d<sub>6</sub>-DMSO)  $\delta$  10.46 (s, 1H); 9.97 (s, 1H); 9.94 (s, 1H); 9.93 (s, 1H); 9.92 (s, 1H); 9.91 (s, 1H); 9.85 (s, 1H); 8.06–8.09 (m, 2H); 7.94–7.96 (m, 2H); 7.39 (s, 1H); 7.29 (s, 1H); 7.24 (bs, 3H); 7.21 (s, 1H); 7.18 (bs, 3H); 7.07 (bs, 3H); 7.04 (s, 1H); 6.98 (s, 1H); 6.91 (s, 1H); 6.89 (s, 1H); 4.59–4.64 (m, 1H); 4.00 (s, 3H); 3.85 (bs, 12H); 3.84 (s, 3H); 3.81 (bs, 6H); 3.21–3.25 (m, 2H); 3.05–3.10 (m, 4H); 2.55–2.57 (m, 2H); 2.34–2.37 (m, 2H); 2.27–2.30 (m, 4H); 2.20 (m, 12H); 1.91 (s, 3H); 1.78–1.80 (m, 2H); 1.53–1.58 (m, 4H). MS calc. 1348.9, exp. 1348.7.

### Compound 4 ImPyPyPy- $\gamma$ -ImPyPyPy-Asp(Dp)-Dp

<sup>1</sup>H NMR (d<sub>6</sub>-DMSO)  $\delta$  10.46 (s, 1H); 10.27 (s, 1H); 9.99 (s, 1H); 9.96 (s, 1H); 9.95 (s, 1H); 9.93 (s, 1H); 9.91 (s, 1H); 8.04–8.09 (m, 2H); 7.90–7.95 (m, 2H); 7.47 (s, 1H); 7.39 (s, 1H); 7.29 (s, 1H); 7.27 (s, 1H); 7.24 (bs, 2H); 7.22 (s, 1H); 7.18 (bs, 3H); 7.15 (s, 1H); 7.07 (s, 1H); 7.04 (s, 1H); 6.97 (s, 1H); 6.90 (s, 1H); 4.59–4.64 (s, 1H); 4.00 (s, 3H); 3.96 (s, 3H); 3.85 (bs, 12H); 3.80 (bs, 6H); 3.20–3.23 (m, 2H); 3.06–3.09 (m, 4H); 2.53–2.55 (m, 2H); 2.35–2.37 (m, 2H); 2.20–2.26 (m, 4H); 2.12 (m, 12H); 1.91 (s, 3H); 1.77–1.80 (m, 2H); 1.51–1.53 (m, 4H). MS calc. 1349.8, exp. 1349.7.

### Compound 5 ImImPyPy- $\gamma$ -PyPyPyPy-Asp(Dp)-Dp

<sup>1</sup>H NMR (d<sub>6</sub>-DMSO)  $\delta$  10.36 (s, 1H); 9.96 (s, 1H); 9.34 (bs, 2H); 9.92 (s, 1H); 9.85 (s, 1H); 9.74 (s, 1H); 8.04–8.07 (m, 2H); 7.92–7.96 (m, 1H); 7.85–7.90 (m, 1H); 7.58 (s, 1H); 7.46 (s, 1H); 7.29 (s, 1H); 7.24 (bs, 2H); 7.23 (s, 1H); 7.18 (bs, 2H); 7.15 (s, 1H); 7.08 (s, 1H); 7.06 (bs, 2H); 6.96 (s, 1H); 6.91 (s, 1H); 6.89 (s, 1H); 4.59–4.62 (s, 1H); 4.01 (bs, 6H); 3.85 (bs, 6H); 3.84 (s, 3H); 3.81 (s, 3H); 3.80 (bs, 6H); 3.23–3.17 (m, 2H); 3.03–3.09 (m, 4H); 2.52–2.55 (m, 2H); 2.27–2.31 (m, 2H); 2.15–2.20 (m, 4H); 2.07 (s, 6H); 2.06 (s, 6H); 1.90 (s, 3H); 1.78–1.82 (m, 2H); 1.47–1.53 (m, 4H).

### Compound 7 ImImPyPy- $\gamma$ -ImPyPyPy-Asp(Dp)-Dp

<sup>1</sup>H NMR (d<sub>6</sub>-DMSO)  $\delta$  10.36 (s, 1H); 10.27 (s, 1H); 9.99 (s, 1H); 9.96 (s, 1H); 9.94 (bs, 2H); 9.73 (s, 1H); 8.04–8.07 (m, 2H); 7.89–7.94 (m, 2H); 7.57 (s, 1H); 7.46 (bs, 2H); 7.28 (bs, 2H); 7.24 (s, 1H); 7.23 (s, 1H); 7.18 (s, 1H); 7.15 (bs, 2H); 7.07 (bs, 2H); 6.96 (s, 1H); 6.90 (s, 1H); 4.59–4.64 (s, 1H); 4.01 (bs, 6H); 3.96 (s, 3H); 3.85 (bs, 9H); 3.80 (bs, 6H); 3.18–3.20 (m, 2H); 3.05–3.08 (m, 4H); 2.53–2.56 (m, 2H); 2.35–2.36 (m, 2H); 2.16–2.20 (m, 4H); 2.07 (m, 12H); 1.90 (s, 3H); 1.78–1.82 (m, 2H); 1.48–1.51 (m, 4H). MS calc. 1350.6, exp. 1350.7.

## Biochemistry

DNase I footprinting was performed according to published protocols [44].

## Fungal Strains

All *Candida* (*C. albicans*, *C. tropicalis*, *C. parapsilosis*), *Cryptococcus* (*C. neoformans*), and *Aspergillus* (*A. niger*) strains were from the American Type Culture Collection (ATCC). Strain numbers are indicated in Figure 2. *Saccharomyces cerevisiae* strains used in ploidy experiments were either from Research Genetics (BY4741, MATa haploid; BY4743, MATa/ $\alpha$  diploid) or ATCC (#204714, MATa/ $\alpha$ / $\alpha$ / $\alpha$  tetraploid). DNA damage hypersensitive yeast mutants were either *rad9::HIS3* (“*rad9*”) or *mec1::TRP1 sm1::HIS3* (“*mec1*”) [45] in the W303 MATa background. Congenic control strains for DNA damage assessment were *RAD9* W303a (“*RAD9*”) or *MEC1 sm1::HIS3* W303a (“*MEC1*”). The collection of *S. cerevisiae* diploid strains heterozygous for essential genes was purchased prearrayed in 96-well plates from Research Genetics.

## In Vitro Susceptibility Testing

In vitro susceptibility testing (MIC) was conducted by the NCCLS broth microdilution assay in 96-well plates [46, 47]. *Saccharomyces cerevisiae* was pregrown on YPD agar plates and tested in YPD media at 30°C. All other strains were pregrown on potato dextrose agar plates tested in RPMI-1640 media at 37°C.

## Acute Fungemia Mouse Model

Compound efficacy in a mouse model of acute fungemia was tested by MDS Pharma Services (Taiwan) using protocol #609010. Groups of 10 ICR derived male mice weighing 22  $\pm$  1 grams were used. Mice were inoculated intravenously (IV) with 10<sup>7</sup> CFU/0.2 ml/mouse



(LD<sub>90-100</sub>) of *Candida albicans* (ATCC 10231) suspended in phosphate-buffered saline (pH 7.4) without mucin. Test compounds (vehicle 0.9% NaCl) were administered intraperitoneally (IP) one hour after the fungal inoculation. Amphotericin B (10 mg/kg) was the reference standard. Mortality was recorded once daily for 10 days.

#### Yeast Heterozygote Hypersensitivity Screen

The collection of diploid *Saccharomyces cerevisiae* strains heterozygous for essential genes was purchased from Research Genetics (release A) as frozen stocks prearrayed on 96-well plates. For the growth hypersensitivity assays, 2  $\mu$ l of thawed glycerol stocks were first inoculated into fresh 96-well plates containing 98  $\mu$ l YPD + 100  $\mu$ g/ml G418 per well and incubated at 30°C for 48 hr to obtain saturated cultures of each strain. Resuspended plates were then diluted 1:10 (10  $\mu$ l to 90  $\mu$ l) into a fresh 96-well plate. This 1:10 dilution was then used as source plate for further dilution (1:5) into daughter plates, which contained either tunicamycin (positive control) or the polyamide of interest at four different (sub-MIC) concentrations. Growth curves were monitored using a system with a Tecan Twister robotic arm integrated with a Tecan Sunrise plate reader in a 30°C warm room. Absorbance (A<sub>600</sub>) was measured every 90 min for 24 hr. Data was parsed and appropriately formatted into MS Excel files using Magellan software. Growth curves were fit using a Boltzman function with initial OD, final OD, slope at midpoint, and time at midpoint as the four parameters used for fitting. As a semiquantitative measure of hypersensitivity, strains which showed growth rates (slope at midpoint) 50%–75% of control (plate average) were scored as having a mild growth defect; 25–50% of control, a moderate growth defect; <25%, a severe defect.

#### Acknowledgments

We acknowledge Jasper Rine for yeast strains and helpful suggestions, and Ken Drazen for support and enthusiasm.

Received: April 22, 2003

Revised: May 28, 2003

Accepted: May 28, 2003

Published: July 18, 2003

#### References

1. Arcamone, F., Penco, S., Orezzi, P.G., Nicoletta, V., and Pirelli, A. (1964). Structure and synthesis of Distamycin A. *Nature* 203, 1064–1065.
2. Arcamone, F., Orezzi, P.G., Barbieri, W., Nicoletta, V., and Penco, S. (1967). Distamycin A. Nota I. Isolamento e struttura dell'agente antivirale distamycin A. *Gazz. Chim. Italiana* 97, 1097–1109.
3. Zimmer, C., and Wahnert, U. (1986). Nonintercalating DNA-binding ligands: Specificity of the interaction and their use as tools in biophysical, biochemical, and biological investigations of the genetic material. *Prog. Biophys. Molec. Biol.* 47, 31–112.
4. Schuhmann, E., Haupt, I., Thrum, H., Taubeneck, U., and May, U. (1974). Effect of distamycin A and netropsin on normal cells and wall-less cells of *Escherichia coli* W 1655 F+. *Zeitschrift für Allg. Mikrobiologie* 14, 321–327.
5. Ginsburg, H., Nissani, E., Krugliak, M., and Williamson, D.H. (1993). Selective toxicity to malaria parasites by non-intercalating DNA-binding ligands. *Mol. Biochem. Parasitol.* 58, 7–15.
6. Thrum, H., Haupt, I., Bradler, G., Zimmer, C.G., and Reinert, K.E. (1972). Antimicrobial and Antineoplastic Chemotherapy 1, 819.
7. Verini, M.A., and Ghione, M. (1964). Activity of distamycin A on vaccinia virus infection of cell cultures. *Chemotherapia* 9, 144–157.
8. Mars, G., and Regoli, U. (1968). Metodo clinico-farmacologico per valutare l'attività antivirale della distamycin A. *Clin. Ter.* 30, 573–580.
9. Burli, R.W., Ge, Y., White, S., Baird, E.E., Touami, S.M., Taylor, M., Kaizerman, J.A., and Moser, H.E. (2002). DNA binding ligands with excellent antibiotic potency against drug-resistant gram-positive bacteria. *Bioorg. Med. Chem. Lett.* 12, 2591–2594.

10. Dyatkina, N.B., Roberts, C.D., Keicher, J.D., Dai, Y., Nadherny, J.P., Zhang, W., Schmitz, U., Kongpachith, A., Fung, K., Novikov, A.A., et al. (2002). Minor groove DNA binders as antimicrobial agents. 1. Pyrrole tetraamides are potent antibacterials against vancomycin resistant *Enterococci* and methicillin resistant *Staphylococcus aureus*. *J. Med. Chem.* 45, 805–817.
11. Lou, L., Velligan, M., Roberts, C., Stevens, D.A., and Clemons, K.V. (2002). DNA binding compounds targeting fungal pathogens: an emerging concept in the discovery of novel antifungal agents. *Curr. Opin. Investig. Drugs* 70, 1437–1445.
12. Lombardi, P., and Crisanti, A. (1997). Antimalarial activity of synthetic analogues of distamycin. *Pharmacol. Ther.* 76, 125–133.
13. Dervan, P.B. (2001). Molecular recognition of DNA by small molecules. *Bioorg. Med. Chem.* 9, 2215–2235.
14. Reddy, B.S., Sharma, S.K., and Lown, J.W. (2001). Recent developments in sequence selective minor groove DNA effectors. *Curr. Med. Chem.* 5, 475–508.
15. Pelton, J.G., and Wemmer, D.E. (1989). Structural characterization of a 2:1 distamycin A.d(CGCAAATTGGC) complex by two-dimensional NMR. *Proc. Natl. Acad. Sci. USA* 15, 5723–5727.
16. Mrksich, M.M., Parks, M.E., and Dervan, P.B. (1994). Hairpin peptide motif. A new class of oligopeptides for sequence-specific recognition in the minor groove of double-helical DNA. *J. Am. Chem. Soc.* 116, 7983–7988.
17. White, S., Szewczyk, J.W., Turner, J.M., Baird, E.E., and Dervan, P.B. (1998). Recognition of the four Watson-Crick base pairs in the DNA minor groove by synthetic ligands. *Nature* 391, 468–471.
18. Kielkopf, C.L., White, S., Sewczyk, J.W., Turner, J.M., Baird, E.E., Dervan, P.B., and Rees, D.C. (1998). A structural basis for recognition of A-T and T-A base pairs in the minor groove of B-DNA. *Science* 282, 111–115.
19. Trauger, J.W., Baird, E.E., and Dervan, P.B. (1998). Cooperative hairpin dimers for recognition of DNA by pyrrole-imidazole polyamides. *Angewandte Chemie* 37, 1421–1423.
20. Trauger, J.W., Baird, E.E., and Dervan, P.B. (1998). Recognition of 16 base pairs in the minor groove of DNA by a pyrrole-imidazole polyamide dimer. *J. Am. Chem. Soc.* 120, 3534–3535.
21. Trauger, J.W., Baird, E.E., and Dervan, P.B. (1996). Recognition of DNA by designed ligands at subnanomolar concentrations. *Nature* 382, 559–561.
22. Gottesfeld, J.M., Neely, L., Trauger, J.W., Baird, E.E., and Dervan, P.B. (1997). Regulation of gene expression by small molecules. *Nature* 387, 202–205.
23. Dickinson, L.A., Gulizia, R.J., Trauger, J.W., Baird, E.E., Mosier, D.E., Gottesfeld, J.M., and Dervan, P.B. (1998). Inhibition of RNA polymerase II transcription in human cells by synthetic DNA-binding ligands. *Proc. Natl. Acad. Sci. USA* 95, 12890–12895.
24. Belitsky, J.M., Leslie, S.J., Arora, P.S., Beerman, T.A., and Dervan, P.B. (2002). Cellular uptake of *N*-Methylpyrrole/*N*-Methylimidazole polyamide-dye conjugates. *Bioorg. Med. Chem.* 10, 3313–3318.
25. Baird, E.E., and Dervan, P.B. (1996). Solid phase synthesis of polyamides containing imidazole and pyrrole amino acids. *J. Am. Chem. Soc.* 118, 6141–6146.
26. Parks, M.E., Baird, E.E., and Dervan, P.B. (1996). Optimization of the hairpin polyamide design for recognition of the minor groove of DNA. *J. Am. Chem. Soc.* 118, 6147–6152.
27. Swalley, E.E., Baird, E.E., and Dervan, P.B. (1999). Effects of  $\gamma$ -turn and  $\beta$ -tail amino acids on the sequence-specific recognition of the minor groove of DNA by hairpin polyamides. *J. Am. Chem. Soc.* 121, 1113–1120.
28. White, S., Baird, E.E., and Dervan, P.B. (1997). Orientation preferences of pyrrole-imidazole polyamides in the minor groove of DNA. *J. Am. Chem. Soc.* 119, 8756–8765.
29. Hawkins, C.A., Pelaez de Clairac, R., Dominey, R.N., Baird, E.E., White, S., Dervan, P.B., and Wemmer, D.E. (2000). Controlling binding orientation in hairpin polyamide DNA complexes. *J. Am. Chem. Soc.* 122, 5235–5243.
30. Bennett, J.E. (1996). Antimicrobial Agents: Antifungal Agents. In *The Pharmacological Basis of Therapeutics* (9<sup>th</sup> edition), Hardman, J.G., Limbird, L.E., Molinoff, P.B., Ruddon, R.W., Gilman, A.G., eds. (New York: McGraw-Hill). CD-ROM.

31. Rine, J. (1991). Gene overexpression in studies of *Saccharomyces cerevisiae*. *Methods Enzymol.* **194**, 239–251.
32. Launhardt, H., Hinnen, A., and Munder, T. (1998). Drug-induced phenotypes provide a tool for the functional analysis of yeast genes. *Yeast* **14**, 935–942.
33. Stori, K., Burckhardt, G., Lown, J.W., and Zimmer, C. (1993). Studies on the ability of minor groove binders to induce supercoiling in DNA. *FEBS Lett.* **334**, 49–54.
34. Kolodner, R.D., Putnam, C.D., and Myung, K. (2002). Maintenance of genome stability in *Saccharomyces cerevisiae*. *Science* **297**, 552–557.
35. Sidorova, J.M., and Breeden, L.L. (1997). Rad53-dependent phosphorylation of Swi6 and down-regulation of *CLN1* and *CLN2* transcription occur in response to DNA damage in *Saccharomyces cerevisiae*. *Genes Dev.* **11**, 3032–3045.
36. Paulovich, A.G., and Hartwell, L.H. (1995). A checkpoint regulates the rate of progression through S-phase in *S. cerevisiae* in response to DNA damage. *Cell* **82**, 841–847.
37. Giaever, G., Shoemaker, D.D., Jones, T.W., Liang, H., Winzeler, E.A., Astromoff, A., and Davis, R.W. (1999). Genomic profiling of drug sensitivities via induced haploinsufficiency. *Nat. Genet.* **21**, 278–283.
38. Barnes, G., Hansen, W.J., Holcomb, C.L., and Rine, J. (1984). Asparagine-linked glycosylation in *Saccharomyces cerevisiae*: genetic analysis of an early step. *Mol. Cell. Biol.* **4**, 2381–2388.
39. Rine, J., Hansen, W., Hardeman, E., and Davis, R.W. (1983). Targeted selection of recombinant clones through gene dosage effects. *Proc. Natl. Acad. Sci. USA* **80**, 6750–6754.
40. Elion, E. (2000). Pheromone response, mating and cell biology. *Curr. Opin. Microbiol.* **3**, 573–581.
41. Naik, R.R., and Jones, E.W. (1998). The *PBN1* gene of *Saccharomyces cerevisiae*: an essential gene that is required for the post-translational processing of the protease B precursor. *Genetics* **149**, 1277–1292.
42. Lai, M.H., Silverman, S.J., Gaughran, J.P., and Kirsch, D.R. (1997). Multiple copies of *PBS2*, *MHP1*, or *LRE1* produce glucanase resistance and other cell wall effects in *Saccharomyces cerevisiae*. *Yeast* **13**, 199–213.
43. Supekova, L., Pezacki, J.P., Su, A.I., Loweth, C.J., Riedl, R., Geierstanger, B., Schultz, P.G., and Wemmer, D.E. (2002). Genomic effects of polyamide/DNA interactions on mRNA expression. *Chem. Biol.* **9**, 821–827.
44. Trauger, J.W., and Dervan, P.B. (2001). Footprinting Methods for Analysis of Pyrrole-Imidazole Polyamide/DNA Complexes. *Methods Enzymol.* **340**, 450–466.
45. Zhao, X., Muller, E.G., and Rothstein, R. (1998). A suppressor of two essential checkpoint genes identifies a novel protein that negatively affects dNTP pools. *Mol. Cell* **2**, 329–340.
46. NCCLS (1997). Reference method for broth dilution antifungal susceptibility testing of yeast. Document M27-A. (NCCLS: Wayne, PA).
47. NCCLS (1997). Reference method for broth dilution antifungal susceptibility testing of filamentous fungi. Document M38-A. (NCCLS: Wayne, PA).